

# Synthesis of Conjugated Polymers Possessing Diketopyrrolopyrrole (DPP) Units Bearing Phenyl, Pyridyl, and Thiazolyl Groups by Direct Arylation Polycondensation: Effects of Aromatic Groups in DPP on Physical Properties

Junpei Kuwabara,<sup>1</sup> Naoto Takase,<sup>1</sup> Takeshi Yasuda,<sup>2</sup> Takaki Kanbara<sup>1</sup>

<sup>1</sup> Tsukuba Research Center for Interdisciplinary Materials Science (TIMS), Graduate School of Pure and Applied Sciences, University of Tsukuba, 1-1-1 Tennodai, Tsukuba, Ibaraki, 305-8573, Japan.

<sup>2</sup> Organic Thin-Film Solar Cells Group, Photovoltaic Materials Unit, National Institute for Materials Science (NIMS), 1-2-1 Sengen, Tsukuba, Ibaraki, 305-0047, Japan.

Correspondence to: T. Kanbara (E-mail: kanbara@ims.tsukuba.ac.jp)

**ABSTRACT:** Conjugated polymers containing phenyl-, pyridyl-, and thiazolyl-flanked diketopyrrolopyrrole (DPP) were synthesized by direct arylation polycondensation of 3,4-ethylenedioxythiophene (EDOT) derivatives and dibrominated DPP-based monomers, in order to probe the effects of the aromatic groups in the DPP units on the absorption property, energy level, and crystallinity. A polymer possessing thiazolyl-flanked DPP units was found to display long-wavelength absorption properties and higher crystallinity than the polymers bearing phenyl- and pyridyl-flanked DPP units. These features of the thiazolyl-based polymer were afforded by its coplanar structure of the main chain. The synthesized polymers showed semiconducting properties in organic field effect transistors (OFETs) and organic photovoltaics (OPVs). Direct arylation polycondensation is an efficient synthetic method that affords a series of DPP-based polymers in a simple fashion and thus helping in a comprehensive understanding on the relationship between the aromatic groups in DPP units and their physical properties.

**KEYWORDS:** conjugated polymer; polycondensation; structure-property relations; direct arylation; diketopyrrolopyrrole (DPP); organic field effect transistors; organic photovoltaics

## INTRODUCTION

Diketopyrrolopyrroles (DPPs) are considered to be one of the most promising units of conjugated polymer materials that are used in organic field effect transistors (OFETs) and organic photovoltaics (OPVs).<sup>1-4</sup> The planar and donor-acceptor structures inherent to DPPs provide aggregation properties, resulting in high carrier mobility in both devices. A choice of aromatic units in DPPs strongly affects the physical properties of DPP-based conjugated polymers.<sup>1-4</sup> Initial investigations focused on phenyl-flanked DPPs,<sup>5</sup> which were derived from a well-known pigment.<sup>6-8</sup> Subsequent investigations focused on thienyl-flanked DPPs because of their higher

degrees of planarity and stronger donor-acceptor properties than those of phenyl-flanked DPPs.<sup>1-4</sup> Along these lines, high-performance conjugated polymers with thieno[3,2-*b*]thiophene,<sup>9,10</sup> pyridyl,<sup>11,12</sup> and thiazolyl-flanked DPPs<sup>13,14</sup> were synthesized and investigated. Among these, the conjugated polymers possessing pyridyl- and thiazolyl-flanked DPPs displayed n-type semiconducting properties owing to the acceptor properties of the pyridyl and thiazolyl groups.<sup>12,14</sup> These DPP-based polymers were originally synthesized by polycondensation using cross coupling reactions between organometallic monomers (organoboron or organotin compounds) and dihalogenated monomers.<sup>1-4</sup> In recent years,

polycondensation using C–H direct arylation has been investigated as an alternative approach,<sup>15–29</sup> and has been successfully applied in the synthesis of DPP-based conjugated polymers by our group<sup>30</sup> and several other groups.<sup>31–37</sup> Because direct arylation polycondensation does not require the preparation of organometallic monomers, a series of conjugated polymers could be synthesized in a simple fashion.<sup>15–19</sup> Herein, we report the synthesis of conjugated polymers containing phenyl-, pyridyl-, and thiazolyl-flanked DPPs by direct arylation polycondensation. We also discuss the effects of aromatic moieties in the DPP units on the absorption property, energy level, and crystallinity.

## EXPERIMENTAL

### Materials

3,4-Ethylenedioxythiophene (EDOT), palladium acetate (Pd(OAc)<sub>2</sub>), and potassium carbonate (K<sub>2</sub>CO<sub>3</sub>) were received from commercial suppliers and used without further purification. Anhydrous dimethylacetamide (DMAc) was purchased from Kanto Chemical and used as a dry solvent. **M1**,<sup>38</sup> **M2**,<sup>39</sup> **M3**,<sup>14</sup> and 3-dihexyl-2,3-dihydro-thieno[3,4-*b*]-1,4-dioxin (dihexylEDOT)<sup>40</sup> were prepared according to the literature methods. Poly(3,4-ethylenedioxythiophene)-poly(styrenesulfonate) (PEDOT:PSS, CLEVIOS P VP AI 4083) was purchased from Heraeus. PC<sub>70</sub>BM (purity 99%) was purchased from Solenne. Standard solutions of Pd (1000 mg L<sup>-1</sup>) was purchased from Kanto Chemical.

### General Measurements and Characterization

NMR spectra were recorded by AVANCE-400 and AVANCE-600 NMR spectrometer (Bruker). Gel permeation chromatography (GPC) measurements were carried out using a prominence GPC system (SHIMADZU) equipped with polystyrene gel columns, using CHCl<sub>3</sub> as the eluent after calibration with polystyrene standards (40 °C). High-temperature GPC measurements were carried out using a HLC-8321 GPC/HT (TOSOH) using *o*-dichlorobenzene (*o*-DCB) as the eluent after calibration with polystyrene standards (140 °C). MALDI-TOF-MS

spectra were recorded on a MALDI TOF/TOF 5800 (AB SCIEX) in a linear mode using *trans*-2-[3-(4-*tert*-Butylphenyl)-2-methyl-2-propenylidene]malononitrile (DCTB) as matrix. The HOMO energy levels were estimated by photoelectron yield spectroscopy (PYS) using an AC-3 spectrometer (Riken Keiki). Ultraviolet-visible (UV-vis) absorption spectra were recorded using a V-630 spectrometer (JASCO). The amounts of residual Pd in the polymers were determined by ICP-MS using an ELAN DRC-e ICP-MS instrument (Perkin Elmer) after decomposing the weighed samples in analytical grade nitric acid with heating. X-ray diffraction patterns were recorded at 298 K on a Rigaku model MultiFlex X-ray diffractometer with a CuK $\alpha$  radiation source. The thermal properties were measured on an EXSTAR TG/DTA6300 instrument. DFT calculations were performed at the B3LYP/6-31G(d) level with the Gaussian09 Rev. D.01 program. All the manipulations for the reactions were carried out under a nitrogen atmosphere using a glove box or standard Schlenk technique. Microwave reactions were conducted using a CEM Discover and Explorer SP System (CEM). The reaction temperature controls were conducted using Dynamic mode of Synergy Software.

### Synthesis of P1

Pd(OAc)<sub>2</sub> (0.56 mg, 2.5  $\mu$ mol) and **M1** (224 mg, 0.25 mmol) were weighed in air and placed in a 10-mL microwave vessel with a magnetic stir bar. The vessel was transferred to a glove box under nitrogen atmosphere. To the microwave vessel, potassium pivalate (87.7 mg, 0.63 mmol), dihexylEDOT (78.8  $\mu$ L, 0.25 mmol), and degassed DMAc (2.5 mL) were added. The vessel was sealed with a septum and taken out from the glove box. The sealed vessel was placed in the microwave reactor and heated at 100 °C for 1 h. After cooling to room temperature, EDOT (13.3  $\mu$ L, 0.13 mmol), Pd(OAc)<sub>2</sub> (0.56 mg, 2.5  $\mu$ mol), and DMAc (0.63 mL) were added to the reaction mixture in the glove box. The mixture was heated at 100 °C for 30 min. After the reaction, an aqueous solution of ethylenediaminetetraacetic acid disodium salt (pH = 8) was added. The suspension was stirred for 2 h at room

temperature. The precipitate was collected by filtration and washed with 0.1 M HCl solution, distilled water, methanol, and hexane. The precipitate was dissolved in  $\text{CHCl}_3$ , and the solution was filtered through Celite to remove insoluble materials. Reprecipitation from chloroform/methanol afforded the polymer as a purple solid. The solid was dispersed in hexane (30 mL) and the suspension was stirred for overnight to remove a low-molecular-weight fraction which was soluble in hexane. The hexane-insoluble fraction was collected by filtration. The solid was dissolved with chloroform and reprecipitation from chloroform/methanol afforded **P1** with a molecular weight of 47300 ( $M_w/M_n = 4.22$ ) in 37% yield.  $^1\text{H}$  NMR (600 MHz,  $\text{C}_2\text{D}_2\text{Cl}_4$ , 120 °C):  $\delta$  7.94 (br, 4H), 7.84 (br, 4H), 4.34 (d,  $J = 7.8$  Hz, 2H), 3.80 (br, 4H), 1.89-1.78 (m, 2H), 1.72-1.11 (m, 68H), 0.94-0.81 (m, 18H).  $^{13}\text{C}\{^1\text{H}\}$  NMR (150 MHz,  $\text{C}_2\text{D}_2\text{Cl}_4$ , 100 °C):  $\delta$  162.66, 147.69, 139.97, 135.52, 128.96, 126.56, 125.68, 115.62, 110.18, 76.92, 45.91, 37.31, 31.47, 31.39, 29.69, 29.29, 29.20, 28.98, 28.76, 28.45, 26.14, 25.53, 22.34, 22.30, 13.69 (6 signals of the alkyl groups were overlapped).

### Synthesis of P2

**P2** was prepared according to the procedure for **P1** using **M2** (224 mg, 0.25 mmol) instead of **M1**.  $M_n = 93700$  ( $M_w/M_n = 3.45$ ), 91% yield.  $^1\text{H}$  NMR (600 MHz,  $\text{C}_2\text{D}_2\text{Cl}_4$ , 100 °C):  $\delta$  9.10 (s, 2H), 9.03 (d,  $J = 7.8$  Hz, 2H), 8.26 (d,  $J = 7.8$  Hz, 2H), 4.37 (br, 6H), 1.87-1.13 (m, 70H), 0.88 (t,  $J = 6.6$  Hz, 6H), 0.83 (t,  $J = 6.6$  Hz, 12H).  $^{13}\text{C}\{^1\text{H}\}$  NMR (150 MHz,  $\text{C}_2\text{D}_2\text{Cl}_4$ , 100 °C):  $\delta$  162.58, 145.68, 145.35, 144.95, 140.93, 132.62, 129.81, 129.82, 127.06, 113.80, 111.52, 77.26, 46.66, 38.26, 31.79, 31.65, 31.56, 31.33, 29.84, 29.45, 29.29, 29.02, 28.75, 28.41, 26.44, 26.40, 25.49, 22.34, 22.25, 13.71, 13.62 (3 signals of the alkyl group were overlapped).

### Synthesis of P3

**P3** was prepared in 0.20 mmol scale according to the procedure for **P1** using **M3** (182 mg, 0.20 mmol) instead of **M1**. DihexyLEDOT (31.5  $\mu\text{L}$ ) was used as an end-capping reagent instead of EDOT. The low-molecular-weight fraction was removed

by washing with hexamethyldisiloxane instead of hexane (30 mL).  $M_n = 23300$  ( $M_w/M_n = 1.74$ ), 63% yield.  $^1\text{H}$  NMR (600 MHz,  $\text{C}_2\text{D}_2\text{Cl}_4$ , 100 °C):  $\delta$  8.19 (s, 2H), 4.43 (br, 2H), 4.31 (br, 4H), 2.00-1.87 (br, 2H), 1.86-1.06 (m, 68H), 0.96-0.70 (m, 18H).  $^{13}\text{C}\{^1\text{H}\}$  NMR (150 MHz,  $\text{C}_2\text{D}_2\text{Cl}_4$ , 100 °C):  $\delta$  160.90, 152.82, 140.19, 139.91, 136.95, 134.34, 110.99, 108.62, 77.98, 46.98, 37.96, 31.79, 31.66, 31.56, 31.39, 31.30, 29.86, 29.46, 29.29, 29.04, 28.72, 28.40, 26.46, 26.39, 25.30, 22.36, 22.30, 22.25, 13.70, 13.67 (1 signal of the alkyl group was overlapped).

### Pd removal procedure

To a solution of **P1** (84.2 mg) in  $\text{CHCl}_3$  (100 mL), a solution of  $\text{NaS}_2\text{CN}(\text{C}_2\text{H}_5)_2$  (20 mg) in water (100 mL) was added. The two-phase mixture was vigorously stirred for 24 h and the organic phase was separated from the aqueous phase and black precipitate composed of Pd. This procedure was repeated again. The organic phase was filtered through Celite and reprecipitation from a chloroform/methanol mixture afforded **P1** (72.8 mg, 86% recovery).

### Fabrication and characterization of OFETs

To estimate the hole mobilities of the polymers, OFETs with a top-contact geometry were fabricated and characterized as follows. A glass/Au gate electrode/Parylene-C insulator substrate was prepared according to the previously reported methods.<sup>41</sup> The **P1–P3** were spin-coated from *o*-DCB solution onto the Parylene-C layer. The coated substrate was then transferred to a  $\text{N}_2$ -filled glove box where it was dried for 10 min at 110 °C. Au (40 nm) source-drain electrodes were thermally evaporated onto the substrates through shadow masks. The channel length and width were fixed at 75  $\mu\text{m}$  and 5 mm, respectively. The OFET measurements were conducted using a Keithley 2636A System Source Meter.

### Fabrication and characterization of OPV cells

The OPV cells were fabricated in the following configuration: ITO/PEDOT:PSS/BHJ layer/LiF/Al. The patterned ITO (conductivity: 10  $\Omega/\text{square}$ ) glass was precleaned in an ultrasonic bath of

acetone and ethanol, and then treated in an ultraviolet-ozone chamber. A thin layer (40 nm) of PEDOT:PSS was spin-coated onto the ITO at 3,000 rpm and air-dried at 110 °C for 10 min on a hot plate. The substrate was then transferred to a N<sub>2</sub>-filled glove box where it was re-dried at 110 °C for 10 min on a hot plate. An *o*-DCB solution of the **P1** and PC<sub>70</sub>BM blended in a 1:3 ratio was subsequently spin-coated onto the PEDOT:PSS surface to form the BHJ layer. The substrates with the BHJ layers were dried for 10 min at 110 °C for the film spin-cast using the *o*-DCB solution. LiF (1 nm) and Al (80 nm) were then deposited onto the active layer by conventional thermal evaporation at a chamber pressure lower than  $5 \times 10^{-4}$  Pa, which provided the devices with an active area of  $5 \times 2$  mm<sup>2</sup>. The thicknesses of BHJ and PEDOT:PSS layers were measured using an automatic microfigure measuring instrument (SURFCORDER ET200, Kosaka Laboratory, Ltd.). The current density-voltage (*J-V*) curves were measured using an ADCMT 6244 DC voltage current source/monitor under AM 1.5 solar-simulated light irradiation of 100 mW cm<sup>-2</sup> (OTENTO-SUN III, Bunkoh-Keiki Co.). The external quantum efficiency (EQE) and the internal quantum

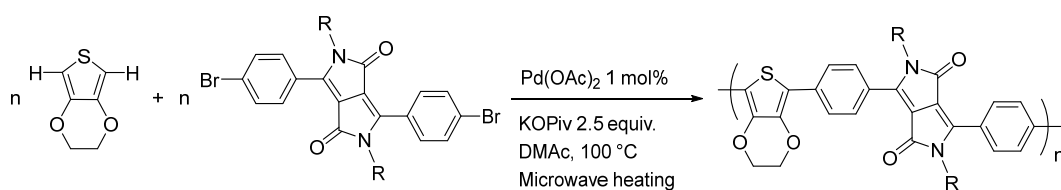
efficiency (IQE) were measured using an SM-250 system (Bunkoh-Keiki Co., Ltd.) with an integrating sphere to determine the reflectance (*R*) of the BHJ OPVs for estimating  $\text{IQE} = \text{EQE} / (1 - R)$ . As a part of the structural characterizations, the surface morphologies were studied using atomic force microscopy (AFM, Nanocute, SII Nano Technology, Inc.).

## RESULTS AND DISCUSSION

### Synthesis of Polymers

Direct arylation polycondensation between dibrominated DPP monomers and EDOT was investigated because the high reactivity of its C–H bond makes it an ideal candidate for direct arylation reactions.<sup>42–47</sup> In addition, EDOT is expected to serve as a strong electron-donor unit in the polymers. Because a combination of direct arylation polycondensation and microwave heating has been reported to afford high-molecular-weight polymers,<sup>45</sup> reaction conditions under microwave heating and the substrate effect of alkyl chains on DPP were investigated in the reaction of EDOT with a dibrominated phenyl-flanked DPP (Table 1).<sup>45</sup>

**TABLE 1** Optimization of reaction conditions and alkyl chains on direct arylation polycondensation of EDOT with dibrominated phenyl-flanked DPPs



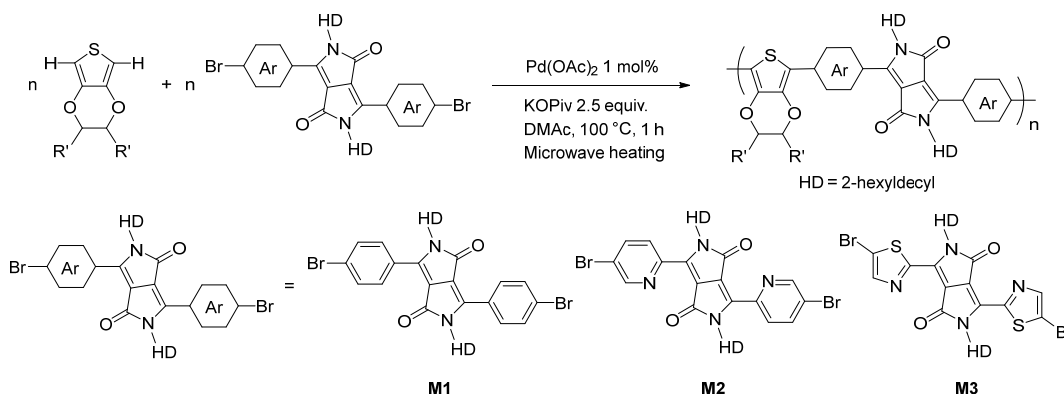
Entry	R <sup>a</sup>	Time / h	Concentration / M	Yield / %	<i>M<sub>n</sub></i>	<i>M<sub>n</sub></i> / <i>M<sub>w</sub></i>
1	OD	0.5 h	0.2	22	4600	1.96
2	OD	1 h	0.2	20	6200	1.78
3 <sup>b</sup>	OD	1 h	0.1	65	15600	2.43
4 <sup>b</sup>	HD	1 h	0.1	87	20400	3.89
5 <sup>b</sup>	EH	1 h	0.1	80	20900	2.82

<sup>a</sup> OD: 2-octyldecyl, HD: 2-hexyldecyl, EH: 2-ethylhexyl. <sup>b</sup> Average of two or more runs.

The reaction of the 2-octyldodecyl-substituted DPP monomer with EDOT afforded an oligomeric product in low yields (Table 1, Entry 1). A longer reaction time did not increase the yield or the molecular weight of the product (Entry 2). However, when the reaction was carried out under a lower concentration of the monomers, both the yield and molecular weight improved (Entry 3). This concentration effect might be explained by the low solubility of the DPP monomer with a long alkyl chain in a polar solvent, *N,N*-dimethylacetamide (DMAc) because the 2-octyldodecyl-substituted DPP monomer was separated from the reaction media as oil

droplet before heating. In terms of the alkyl chains, the 2-hexyldodecyl group appeared to be the optimal chain length among the three (i.e., 2-octyldodecyl, 2-hexyldodecyl, and 2-ethylhexyl) in both yield and molecular weight (Entries 3–5). The molecular weight of 20400 is also comparable to that of the same polymer recently synthesized by polycondensation using the Migita–Kosugi–Stille coupling reaction ( $M_n = 16700$ ).<sup>48</sup> It should be noted that only 1 mol% of the Pd catalyst is needed and the polymer is obtained within 1 h, presumably owing to uniform and rapid microwave heating.<sup>45,49</sup>

**TABLE 2** Results of Polycondensation



Entry	R'	Monomer	Polymer	Yield / %	$M_n$	$M_w/M_n$	Pd residue <sup>a</sup> / ppm
1 <sup>b</sup>	H	<b>M1</b>		94	20400	3.89	- <sup>c</sup>
2	H	<b>M2</b>		94	22300	6.90	- <sup>c</sup>
3	H	<b>M3</b>		71	1200	9.51	- <sup>c</sup>
4	C <sub>6</sub> H <sub>13</sub>	<b>M1</b>	<b>P1</b>	37 <sup>d</sup>	47300 (7800) <sup>f</sup>	4.22 (4.58) <sup>f</sup>	41
5	C <sub>6</sub> H <sub>13</sub>	<b>M2</b>	<b>P2</b>	91 <sup>d</sup>	93700 (60100) <sup>f</sup>	3.45 (2.75) <sup>f</sup>	372
6	C <sub>6</sub> H <sub>13</sub>	<b>M3</b>	<b>P3</b>	63 <sup>e</sup>	23300 (17500) <sup>f</sup>	1.74 (1.68) <sup>f</sup>	304

<sup>a</sup> Measured by ICP-MS after washing with aqueous solution of Na<sub>2</sub>CN(C<sub>2</sub>H<sub>5</sub>)<sub>2</sub>, <sup>b</sup> Table 1, Entry 4, <sup>c</sup> Not determined, <sup>d</sup> Yield after washing with hexane, <sup>e</sup> Result after washing with hexamethyldisiloxane. <sup>f</sup> Results in parentheses were obtained from high-temperature GPC (*o*-dichlorobenzene, 140 °C).

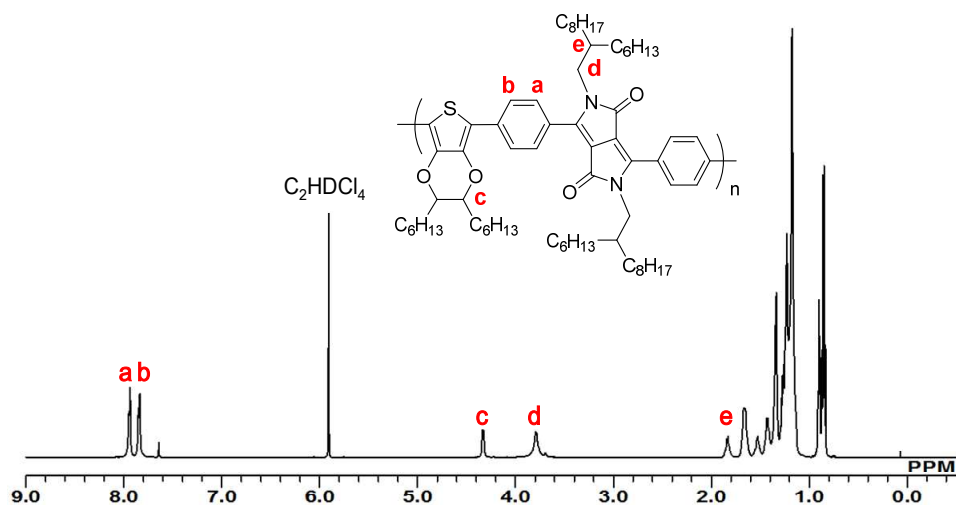


**FIGURE 1**  $^1\text{H}$  NMR spectrum of **P1** (600 MHz in  $\text{C}_2\text{D}_2\text{Cl}_4$  at 393K).

The reactions of pyridyl- and thiazolyl-flanked DPPs with EDOT were conducted under the optimized reaction conditions for the phenyl-flanked DPP monomer (Table 2, Entries 1–3). The polycondensation reaction of the pyridyl-flanked DPP monomer (**M2**) afforded the corresponding polymer in a good yield (Entry 2). However, the reaction of the thiazolyl-flanked DPP monomer (**M3**) afforded only oligomeric products (Entry 3). Because the low solubility of the formed polymer was considered to prohibit the propagation reaction, an alkylated EDOT ( $\text{R}' = \text{C}_6\text{H}_{13}$ , dihexyleDOT) was used in the reaction with **M1–M3** under the same reaction conditions (Entries 4–6) in order to obtain a higher-molecular-weight product.<sup>39,50</sup> The introduction of the hexyl groups dramatically increased the solubility of polymers in organic solvents; most of the polymer (**P1**) produced from dihexyleDOT and **M1** was hexane soluble. Therefore, the yield of **P1** after washing with hexane was 37% (Entry 4). The reactions of **M2** or **M3** with dihexyleDOT afforded higher-molecular-weight polymers than their corresponding EDOT-based polymers (Entries 5 and 6). In contrast to successful polymerization of **M2** and **M3**, the reaction with a thienyl-flanked DPP afforded insoluble products presumably due to a cross-linking side reaction at the undesired C-H moiety in the thienyl group.<sup>22</sup> The  $^1\text{H}$  NMR spectrum of **P1** shows

sharp signals corresponding to the repeating units at 120 °C (Fig. 1), while broad signals are predominant at room temperature owing to aggregation (Fig. S-4). The signals at 7.64 ppm can be assigned to the protons of the brominated phenyl group in the terminal DPP unit (Fig. S-4). This observation is further supported by the MALDI–TOF–MS results of **P1** (Fig. S-6). The MS spectrum also indicates the presence of a small amount of defects caused by a homo coupling reaction of dihexyleDOT.<sup>51–53</sup> To evaluate the aggregation effect on the GPC measurements, high-temperature GPC measurements (140 °C) were conducted in addition to the normal GPC measurements (40 °C) (Table 2). Because the high-temperature GPC shows smaller molecular weight than those from the normal GPC, the aggregation effects are considered to induce overestimation of the molecular weight of the polymers. The structures of **P2** and **P3** were also characterized by  $^1\text{H}$  NMR,  $^{13}\text{C}\{^1\text{H}\}$  NMR, and MALDI–TOF–MS (Fig. S-7–S1-2). The Pd catalyst residue was removed from **P1–P3** by washing with an aqueous solution of sodium *N,N*-diethyldithiocarbamate ( $\text{NaS}_2\text{CN}(\text{C}_2\text{H}_5)_2$ ) at room temperature.<sup>54,55</sup> Residual amounts of Pd were measured by ICP–MS. After purification, the residual amount of Pd in **P1** was 41 ppm, which was significantly higher than that of the EDOT–fluorene polymer (**P0**, 2.4 ppm, Fig. 2),

which was purified by the same method.<sup>55</sup> Moreover, **P2** and **P3** contained even more Pd residue (372 and 304 ppm) after purification. The difficulties in removing the Pd catalyst residue from these polymers (**P1**, **P2**, and **P3**) could be explained by the presence of several coordination sites such as the carbonyl group and imine nitrogen.

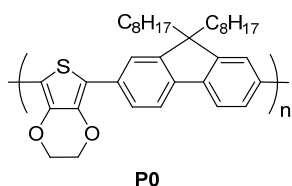


**FIGURE 2** The chemical structure of the reference polymer.

### Physical Properties

The UV-vis absorption spectra of **P1–P3** and the reference polymer (**P0**)<sup>46</sup> are shown in Fig. 3. For all the four polymers, the solution phase and film state absorption spectra were similar to each other. Owing to the presence of DPP units, **P1–P3** show long-wavelength absorption compared to **P0**: the absorption coefficients of **P0–P3** are in the same range (Table S-1). Absorption region clearly depends on the aromatic groups of the DPP units. The order of maximum absorption wavelength ( $\lambda_{max}$ ) is **P1** < **P2** < **P3**. The comparison of the physical properties of a pyridyl-containing DPP polymer and that of a thiazolyl-containing DPP polymer have not yet been reported. Therefore, we further investigated the difference in the absorption properties by using the results of density-functional theory (DFT) calculations. Energy-minimized structures of the modeling compounds for **P1–P3** are shown in Fig. 4. The result shows that **P1** has large dihedral angles around the phenyl moiety (23.82° and 14.32°).<sup>2</sup>

In the case of **P2**, the dihedral angle between the pyridyl moiety and the DPP core decreases to 0.17° owing to less steric hindrance caused by the N moiety in the pyridyl unit versus the C–H group in the phenyl unit.<sup>12</sup> Moreover, **P3** also has a small dihedral angle between the thiazolyl and EDOT units (0.23°), presumably due to the low steric hindrance of a five-membered thiazolyl ring. In addition, an intramolecular S···O interaction may also contribute to the planner structure of **P3**.<sup>56</sup> Coplanarity of the main chain structures is likely to affect the absorption properties.

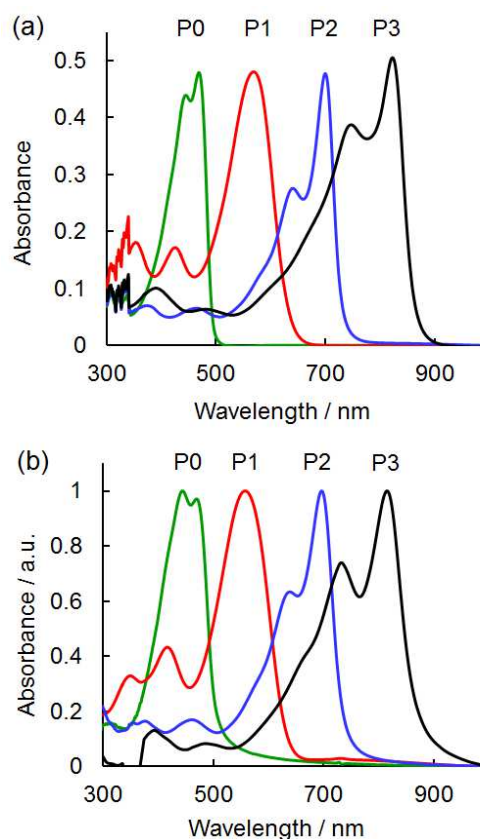


**FIGURE 3** UV-vis absorption spectra of **P0–P3** (a) in  $\text{CHCl}_3$  ( $1.0 \times 10^{-5}$  M) and (b) in the film state.

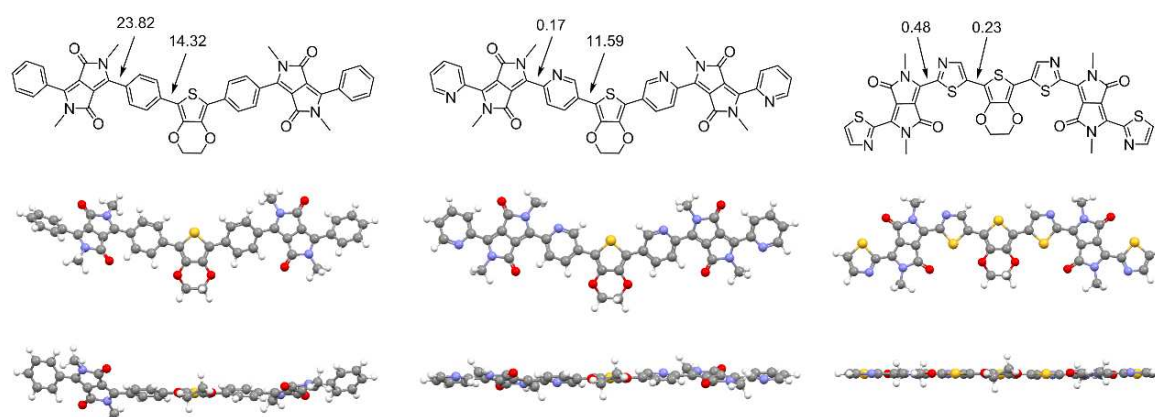


**FIGURE 4** Energy-minimized structures of the model compounds for **P1**, **P2**, and **P3** obtained by DFT calculations at a B3LYP 6-31G(d) level.

**TABLE 3** Physical properties and energy levels of polymers

Polymer	$\lambda_{\max}^a$ / nm	$\lambda_{\max}^b$ / nm	$E_g^{\text{opt}c}$ / eV	HOMO <sup>d</sup> / eV	LUMO <sup>e</sup> / eV	$T_d^f$ / °C
<b>P1</b>	568	558	1.98	-5.34	-3.36	343
<b>P2</b>	700	696	1.70	-5.46	-3.76	334
<b>P3</b>	822	814	1.44	-5.23	-3.79	347

<sup>a</sup> In CHCl<sub>3</sub> (1.0 × 10<sup>-5</sup> M). <sup>b</sup> In the film state. <sup>c</sup> Estimated from the absorption onset in the film state. <sup>d</sup> Estimated from PYS. <sup>e</sup>  $E_{\text{LUMO}} = E_g^{\text{opt}} + E_{\text{HOMO}}$ . <sup>f</sup> The 5% weight-loss temperature under inert atmosphere.

To investigate the electronic effects of the aromatic group, HOMO and LUMO energy levels were determined by the results of PYS and optical bandgaps (Table 3). The deep HOMO level of **P2** is due to the strong acceptor property of the pyridyl group.<sup>12</sup> Although the thiazolyl group is also known to act as an acceptor unit,<sup>14</sup> the HOMO level of **P3** is the highest among the three polymers. DFT calculations suggest that the HOMO of **P3** is delocalized over all units, while the HOMO of **P2** is localized on the EDOT and DPP cores (Fig. S-13). Therefore, the efficient conjugation on the main chain in **P3** is responsible for the lower band gap and the higher HOMO level than **P2**.

### X-Ray Diffraction (XRD) Analysis

The crystallinity of **P1–P3** was evaluated by XRD analysis before and after thermal annealing at 200 °C (Fig. 5 and Table 4). The XRD patterns of **P1–P3** exhibited diffraction peaks with a scattering angle ( $2\theta$ ) of around 6°, which could be assigned to diffractions arising from lamellar structures. In addition, relatively weak diffractions were observed around 21°–23°, corresponding to a  $\pi$ – $\pi$  stacking distance. The thermal annealing treatments expanded the lamellar distances and shortened the  $\pi$ – $\pi$  stacking distances. The lamellar peak in **P3** was significantly sharpened by thermal annealing in comparison to **P1** and **P2**, presumably owing to the coplanar structure of the main chain in **P3**. The crystalline nature of **P1–P3** is in sharp contrast to the amorphous nature of **P0**.<sup>46</sup>

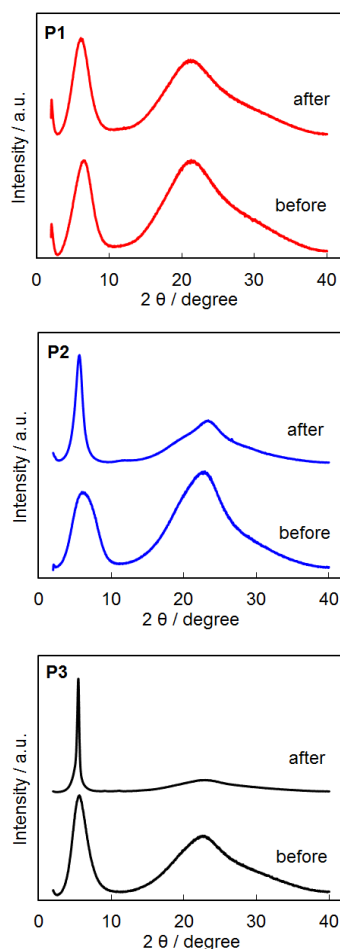


**FIGURE 5** X-ray diffraction patterns of **P1–P3** before and after annealing at 200 °C.

### OFETs and OPV Properties

**P1–P3** were evaluated for their semiconducting properties in OFETs and OPVs. The details of the OFET and OPV fabrication are described in the experimental section. The OFETs showed moderate field-effect hole mobilities ( $\mu_h$ ) in **P1–P3** (Table 5). Bulk heterojunction (BHJ) OPVs were fabricated with **P1** and PC<sub>70</sub>BM on several blend ratios with various thicknesses (Table 6 and S-2). The OPV fabricated using **P1**:PC<sub>70</sub>BM at a 1:3 mixing ratio with thickness 110 nm yielded the PCE of 0.96% (Table 6, Entry 1). The PCEs increased as the thickness decreased (Entries 2 and 3). The surface morphology of the active layers was evaluated by AFM (Fig. 6). In comparison with a smooth surface of **P1** (Fig. 6a), a BHJ film with **P1** and PC<sub>70</sub>BM was found to be more rough, indicating a substantial phase separation (Fig. 6b). The addition of 3% 1,8-diodooctane (DIO) in *o*-DCB decreased the domain size (Fig. 6c). On decreasing the domain size by adding DIO, the PCE slightly increased to 2.20% (Table 6, Entry 4). Both **P2** and **P3** show strong aggregation behavior, and hence, they are unsuitable for obtaining appropriate phase separation (Fig. S-18).

**TABLE 4** Results of XRD measurements

Polymer	2θ / rad.	<i>d</i> -spacing / Å	Harf-value width <sup>a</sup> / rad.
P1	6.49, 21.31	13.60, 4.16	3.66
P1-annealed <sup>b</sup>	6.11, 21.42	14.46, 4.15	3.22
P2	6.18, 21.31	14.32, 3.96	3.78
P2-annealed <sup>b</sup>	5.66, 23.61	15.62, 3.77	1.30
P3	5.62, 22.54	15.73, 3.94	2.64
P3-annealed <sup>b</sup>	5.47, 22.74	16.14, 3.91	0.37

<sup>a</sup> Harf-value width of the first diffraction peak. <sup>b</sup> Annealed at 200 °C for 30 min under N<sub>2</sub>.

**TABLE 5** OFET characteristics<sup>a</sup>

Polymer	$\mu_h^b / \text{cm}^2\text{V}^{-1}\text{s}^{-1}$	on/off ratio	$V_{th}^c / \text{V}$
<b>P1</b>	$5.6 \pm 0.8 \times 10^{-5}$	$1.3 \pm 0.2 \times 10^3$	$-33 \pm 4$
<b>P2</b>	$2.2 \pm 0.9 \times 10^{-4}$	$2 \pm 1 \times 10^3$	$-52 \pm 2$
<b>P3</b>	$7.3 \pm 0.3 \times 10^{-5}$	$1.1 \pm 0.3 \times 10^3$	$-36 \pm 3$

<sup>a</sup> The average values with standard deviations were calculated from the results of three or more OFET samples. OFET configuration; Glass/Au gate electrode/Parylene-C insulator/Polymer/Au source-drain electrodes. <sup>b</sup> Field-effect hole mobility. <sup>c</sup> Threshold voltage.

**TABLE 6** OPV characteristics of **P1**<sup>a</sup>

Entry	Thickness	Additive	$J_{sc}^b / \text{mAcm}^{-2}$	$V_{oc}^b / \text{V}$	$FF^b$	$\text{PCE}^b / \%$
1	111		2.33	0.90	0.46	$0.96 \pm 0.04$
2	82		3.43	0.90	0.50	$1.55 \pm 0.06$
3	55		4.16	0.86	0.56	$2.01 \pm 0.17$
4	57	DIO <sup>c</sup>	4.63	0.88	0.54	$2.20 \pm 0.07$

<sup>a</sup> OPV configuration; ITO/PEDOT:PSS (40 nm)/**P1**:PC<sub>70</sub>BM(1:3)/LiF(1 nm)/Al(80 nm). Illuminated at 100 mWcm<sup>-2</sup> of AM 1.5; <sup>b</sup> Average values at least 3 runs; <sup>c</sup> 3 vol% 1,8-diiodooctane (DIO).

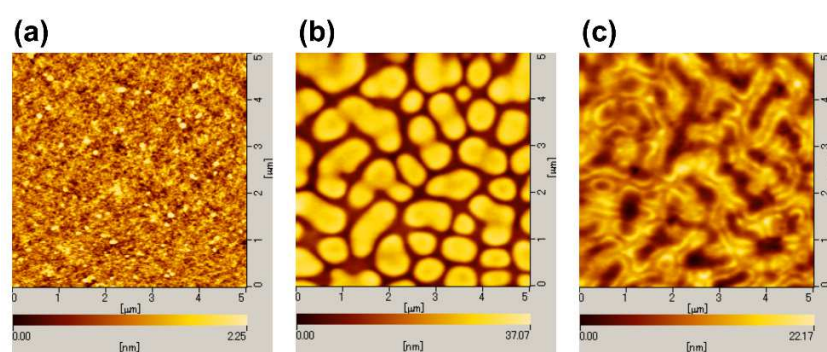


**FIGURE 6** AFM images ( $5 \times 5 \mu\text{m}^2$ ) of thin films of (a) **P1** (RMS: 0.3585 nm), (b) **P1**:PC<sub>70</sub>BM (1:3) (RMS: 8.745 nm) fabricated by spin coating from *o*-DCB solution, and (c) **P1**:PC<sub>70</sub>BM (1:3) (RMS: 3.652 nm) fabricated by spin coating from *o*-DCB solution containing 3% DIO.

## CONCLUSION

Three kinds of DPP-based conjugated polymers were synthesized by direct arylation polycondensation under microwave heating. The high reactivity of the C–H bond in the EDOT derivative enabled smooth direct arylation polycondensation with dibrominated DPP-based monomers bearing different aromatic units, which showed semiconducting behavior in OFETs and OPVs. In terms of purification of the obtained polymers, the efficiency of the removal of a Pd residue depends on the chemical structure of the polymers; coordination sites such as a carbonyl group and imine nitrogen make the Pd removal difficult. The polymer with a thiazolyl-flanked DPP unit shows long-wavelength absorption compared to phenyl- and pyridyl-flanked DPP units. DFT calculation showed that the characteristic physical properties of the thiazolyl-DPP polymer were caused by the delocalization of HOMO over all units owing to its coplanar structure of the main chain. The efficient synthetic method, direct arylation polycondensation, provided a series of DPP-based polymers in a simple fashion, leading to a comprehensive understanding of the effects of the aromatic group of the DPP unit on their physical properties. These insights provide important information for the molecular design of DPP-based polymers.

## ACKNOWLEDGEMENTS

The authors thank the Chemical Analysis Center of University of Tsukuba for the measurements of NMR spectra, MALDI-TOF-MS, and ICP-MS. The authors also thank to Prof. Y. Nishihara and Prof. H. Mori of Okayama University for the measurement of high-temperature GPC, and Prof. T. Koizumi and the Center for Advanced Materials Analysis, Technical Department, Tokyo Institute of Technology for the elemental analyses. The authors wish to thank Prof. S. Kagaya of University of Toyama for valuable advices for measurements of ICP-MS. This work was supported by Industrial Technology Research Grant Program in 2011 from New Energy and Industrial Technology Development Organization

(NEDO) of Japan, and partly supported by Grant-in-Aid for Grant-in-Aid for Young Scientists (B) (15K17922), Challenging Exploratory Research (25620094) and Scientific Research (B) (25288052).

## REFERENCES

1. Y. Li, P. Sonar, L. Murphy, W. Hong, *Energy Environ. Sci.* **2013**, *6*, 1684–1710.
2. C. B. Nielsen, M. Turbiez, I. McCulloch, *Adv. Mater.* **2013**, *25*, 1859–1880.
3. M. A. Naik, S. Patil, *J. Polym. Sci. Part A: Polym. Chem.* **2013**, *51*, 4241–4260.
4. W. Li, K. H. Hendriks, M. M. Wienk, R. A. J. Janssen, *Acc. Chem. Res.* **2016**, *49*, 78–85.
5. B. Tieke, A. R. Rabindranath, K. Zhang, Y. Zhu, *Beilstein J. Org. Chem.* **2010**, *6*, 830–845.
6. Z. Hao, A. Iqbal, *Chem. Soc. Rev.* **1997**, *26*, 203–213.
7. M. Grzybowski, D. T. Gryko, *Adv. Optical Mater.* **2015**, *3*, 280–320.
8. J. Kuwabara, T. Yamagata, T. Kanbara, *Tetrahedron*, **2010**, *66*, 3736–3741.
9. H. Bronstein, Z. Chen, R. S. Ashraf, W. Zhang, J. Du, J. R. Durrant, P. S. Tuladhar, K. Song, S. E. Watkins, Y. Geerts, M. M. Wienk, R. A. J. Janssen, T. Anthopoulos, H. Sirringhaus, M. Heeney, I. McCulloch, *J. Am. Chem. Soc.* **2011**, *133*, 3272–3275.
10. R. S. Ashraf, I. Meager, M. Nikolka, M. Kirkus, M. Planells, B. C. Schroeder, S. Holliday, M. Hurhangee, C. B. Nielsen, H. Sirringhaus, I. McCulloch, *J. Am. Chem. Soc.* **2015**, *137*, 1314–1321.
11. J. W. Jung, F. Liu, T. P. Russell, W. H. Jo, *Chem. Commun.* **2013**, *49*, 8495–8497.
12. B. Sun, W. Hong, Z. Yan, H. Aziz, Y. Li, *Adv. Mater.* **2014**, *26*, 2636–2642.
13. B. Carsten, J. M. Szarko, L. Lu, H. J. Son, F. He, Y. Y. Botros, L. X. Chen, L. Yu, *Macromolecules* **2012**, *45*, 6390–6395.

14. W. Li, W. S. C. Roelofs, M. Turbiez, M. M. Wienk, R. A. J. Janssen, *Adv. Mater.* **2014**, *26*, 3304–3309.
15. S. Kowalski, S. Allard, K. Zilberberg, T. Riedl, U. Scherf, *Prog. Polym. Sci.* **2013**, *38*, 1805–1814.
16. L. G. Mercier, M. Leclerc, *Acc. Chem. Res.* **2013**, *46*, 1597–1605.
17. K. Okamoto, J. Zhang, J. B. Housekeeper, S. R. Marder, C. K. Luscombe, *Macromolecules* **2013**, *46*, 8059–8078.
18. J. Kuwabara, T. Kanbara, *J. Synth. Org. Chem. Jpn.* **2014**, *72*, 1271–1277.
19. A. E. Rudenko, B. C. Thompson, *J. Polym. Sci., Part A: Polym. Chem.* **2015**, *53*, 135–147.
20. Q. Wang, R. Takita, Y. Kikuzaki, F. Ozawa, *J. Am. Chem. Soc.* **2010**, *132*, 11420–11421.
21. W. Lu, J. Kuwabara, T. Kanbara, *Macromolecules* **2011**, *44*, 1252–1255.
22. Y. Fujinami, J. Kuwabara, W. Lu, H. Hayashi, T. Kanbara, *ACS Macro Lett.* **2012**, *1*, 67–70.
23. P. Berrouard, A. Najari, A. Pron, D. Gendron, P.-O. Morin, J.-R. Pouliot, J. Veilleux, M. Leclerc, *Angew. Chem., Int. Ed.* **2012**, *51*, 2068–2071.
24. S. Kowalski, S. Allard, U. Scherf, *ACS Macro Lett.* **2012**, *1*, 465–468.
25. S.-W. Chang, H. Waters, J. Kettle, Z.-R. Kuo, C.-H. Li, C.-Y. Yu, M. Horie, *Macromol. Rapid Commun.* **2012**, *33*, 1927–1932.
26. M. Wakioka, N. Ichihara, Y. Kitano, F. Ozawa, *Macromolecules* **2014**, *47*, 626–631.
27. A. E. Rudenko, B. C. Thompson, *Macromolecules* **2015**, *48*, 569–575.
28. R. Matsidik, H. Komber, A. Luzio, M. Caironi, M. Sommer, *J. Am. Chem. Soc.* **2015**, *137*, 6705–6711.
29. T. Bura, P.-O. Morin, M. Leclerc, *Macromolecules* **2015**, *48*, 5614–5620.
30. J. Kuwabara, Y. Nohara, S. J. Choi, Y. Fujinami, W. Lu, K. Yoshimura, J. Oguma, K. Suenobu, T. Kanbara, *Polym. Chem.* **2013**, *4*, 947–953.
31. Q. Guo, J. Dong, D. Wan, D. Wu, J. You, *Macromol. Rapid Commun.* **2013**, *34*, 522–527.
32. J.-R. Pouliot, L. G. Mercier, S. Caron, M. Leclerc, *Macromol. Chem. Phys.* **2013**, *214*, 453–457.
33. J.-R. Pouliot, B. Sun, M. Leduc, A. Najari, Y. Li, M. Leclerc, *Polym. Chem.* **2014**, *6*, 278–282.
34. Y. Gao, X. Zhang, H. Tian, J. Zhang, D. Yan, Y. Geng, F. Wang, *Adv. Mater.* **2015**, *27*, 6753–6759.
35. P. Homyak, Y. Liu, F. Liu, T. P. Russel, E. B. Coughlin, *Macromolecules* **2015**, *48*, 6978–6986.
36. S. Broll, F. Nübling, A. Luzio, D. Lentzas, H. Komber, M. Caironi, M. Sommer, *Macromolecules* **2015**, *48*, 7481–7488.
37. K. Wang, G. Wang, M. Wang, *Macromol. Rapid Commun.* **2015**, *36*, 2162–2170.
38. S.-Y. Liu, M.-M. Shi, J.-C. Huang, Z.-N. Jin, X.-L. Hu, J.-Y. Pan, H.-Y. Li, A. K.-Y. Jen, H.-Z. Chen, *J. Mater. Chem. A* **2013**, *1*, 2795–2805.
39. C. J. Mueller, C. R. Singh, M. Fried, S. Huettnner, M. Thelakkat, *Adv. Funct. Mater.* **2015**, *25*, 2725–2736.
40. D. Caras-Quintero, P. Bäuerle, *Chem. Commun.* **2004**, 926–927.
41. T. Yasuda, Y. Shinohara, T. Matsuda, L. Han, T. Ishi-i, *J. Polym. Sci. Part A: Polym. Chem.* **2013**, *15*, 2536–2544.
42. A. Kumar, A. Kumar, *Polym. Chem.* **2010**, *1*, 286–288.
43. K. Yamazaki, J. Kuwabara, T. Kanbara, *Macromol. Rapid Commun.* **2013**, *34*, 69–73.
44. L. A. Estrada, J. J. Deininger, G. D. Kamenov, J. R. Reynolds, *ACS Macro Lett.* **2013**, *2*, 869–873.
45. S. J. Choi, J. Kuwabara, T. Kanbara, *ACS Sustainable Chem. Eng.* **2013**, *1*, 878–882.
46. J. Kuwabara, T. Yasuda, S. J. Choi, W. Lu, K. Yamazaki, S. Kagaya, L. Han, T. Kanbara, *Adv. Funct. Mater.* **2014**, *24*, 3226–3233.

47. S. Hayashi, T. Koizumi, *Polym. Chem.* **2015**, *6*, 5036–5039.
48. C. J. Mueller, C. R. Singh, M. Thelakkat, *J. Polym. Sci. Part B: Polym. Phys.* **2016**, *54*, 639–648.
49. C. O. Kappe, *Angew. Chem., Int. Ed.* **2004**, *43*, 6250–6284.
50. W. Lu, J. Kuwabara, M. Kuramochi, T. Kanbara, *J. Polym. Sci. Part A: Polym. Chem.* **2015**, *53*, 1396–1402.
51. F. Lombeck, H. Komber, S. I. Gorelsky, M. Sommer, *ACS Macro Lett.* **2014**, *3*, 819–823.
52. S. Kowalski, S. Allard, U. Scherf, *Macromol. Rapid Commun.* **2015**, *36*, 1061–1068.
53. J. Kuwabara, M. Sakai, Q. Zhang, T. Kanbara, *Org. Chem. Front.* **2015**, *2*, 520–525.
54. K. T. Nielsen, H. Spanggaard, F. C. Krebs, *Macromolecules* **2005**, *38*, 1180–1189.
55. J. Kuwabara, T. Yasuda, N. Takase, T. Kanbara, *ACS Appl. Mater. Interfaces* **2016**, *8*, 1752–1758.
56. C. Bleiholder, R. Gleiter, D. B. Werz, H. Köppel, *Inorg. Chem.* **2007**, *46*, 2249–2260.

**GRAPHICAL ABSTRACT**

## AUTHOR NAMES

Junpei Kuwabara, Naoto Takase, Takeshi Yasuda, Takaki Kanbara

## TITLE

Synthesis of Conjugated Polymers Possessing Diketopyrrolopyrrole (DPP) Units Bearing Phenyl, Pyridyl, and Thiazolyl Groups by Direct Arylation Polycondensation: Effects of Aromatic Groups in DPP on Physical Properties

## TEXT

Direct arylation polycondensation of an EDOT derivative with dibrominated diketopyrrolopyrrole (DPP) monomers afforded conjugated polymers containing phenyl-, pyridyl-, and thiazolyl-flanked DPP units. Investigation on their physical properties revealed the effects of the aromatic group in the DPP units. The polymer bearing the thiazolyl-flanked DPP unit has a long-wavelength absorption property and high crystallinity owing to a coplanar structure of a main chain, compared with the polymers bearing phenyl- and pyridyl-flanked DPP units.

**Graphical Abstract for Table of Contents**